Diagn Interv Radiol 2009; 15:121–126
© Turkish Society of Radiology 2009

Radiologic findings in malignant gastrointestinal stromal tumors

Şerife Ulusan, Zafer Koç

ABSTRACT
In this pictorial essay, we describe the computed tomographic and magnetic resonance imaging appearances of primary and metastasized gastrointestinal stromal tumors. These nonepithelial tumors arise from the muscularis propria in the wall of the gastrointestinal tract and are thought to originate from Cajal cells in the interstitium of intestinal pacemaker tissue. These tumors are found in the stomach, small bowel, colon, rectum, and esophagus; they may also develop as primary tumors of the omentum, mesentery, or retroperitoneum. The clinical features and radiologic differential diagnosis of gastrointestinal stromal tumors are discussed.

Key words: • *gastrointestinal stromal tumors* • *computed tomography* • *magnetic resonance imaging*

From the Department of Radiology (Ş.U. ✉ *sulusan@hotmail.com*), Başkent University School of Medicine, Adana, Turkey.

Received 21 May 2007; revision requested 21 October 2007; revision received 21 November 2007; accepted 25 December 2007.

Gastrointestinal stromal tumors (GISTs) are rare (1) but are the most common mesenchymal neoplasms in the gastrointestinal (GI) tract. These nonepithelial tumors arise from the muscularis propria in the wall of the GI tract and are thought to originate from Cajal cells in the interstitium of intestinal pacemaker tissue (1, 2) (Fig. 1). The most frequent site of occurrence is the stomach (60% of all cases) (Fig. 2), followed by the small bowel (30%) (Fig. 3), and other sites (colon and rectum, 5%) (Fig. 4), and the esophagus (<5%) (1–4). GISTs also may develop as primary tumors of the omentum, mesentery, or retroperitoneum. They account for 1% to 3% of all gastric neoplasms, 20% of all small bowel tumors, and 0.2% to 1% of all colorectal tumors (1–5). Earlier medical reports refer to these tumors as leiomyomas, leiomyoblastomas, leiomyosarcomas, or schwannomas. However, in 1983, electron microscopy and immunohistochemistry studies revealed that these lesions contain no smooth muscle or Schwann cells, so the nomenclature was changed to GIST.

GISTs are classified as spindle cell, epithelioid, or pleomorphic mesenchymal tumors of the GI tract (1–5). All express KIT protein (CD117 stem cell factor receptor), which can be detected immunohistochemically (1–5). KIT is a type-3 receptor tyrosine kinase that is important for the development of melanocytes, germ cells, mast cells, hematopoietic stem cells, interstitial cells of Cajal, and the pacemaker cells of the GI tract that GIST cells most closely resemble. KIT-activating mutations are found in 85% to 90% of GISTs (6). In recent years, immunohistochemical staining for KIT (CD117) has become integral to the diagnosis of GISTs, nearly 90% of which harbor activating mutations in the KIT receptor tyrosine kinase gene. Approximately 80% of patients with metastatic GISTs show at least some clinical response to the targeted small-molecule KIT inhibitor, imatinib (6). The response to imatinib is closely correlated with the presence and type of KIT mutation. GISTs with the most common KIT exon 11 mutations have the highest response rate by far, whereas GISTs lacking mutations in KIT or the alternative receptor tyrosine kinase PDGFRA (platelet-derived growth factor receptor) show much lower rates of response to imatinib. Less than 5% of GISTs are KIT-immunonegative, and many of these tumors have activating mutations of PDGFRA, some of which are also inhibited by imatinib (6).

Seventy percent to 80% of GISTs are benign, and such tumors are often found incidentally at surgery and excised in the same session. Approximately 20% to 30% of GISTs are malignant, and these neoplasms are identified based on their mitotic index, tumor necrosis index, and Ki-67 index (which reflects expression of the 395 kDa nuclear antigen MIB-1). According to recent pathological studies, high values for these parameters are the most important prognostic factors for metastasis and mortality in this patient population (1–5). Some characteristic comput-

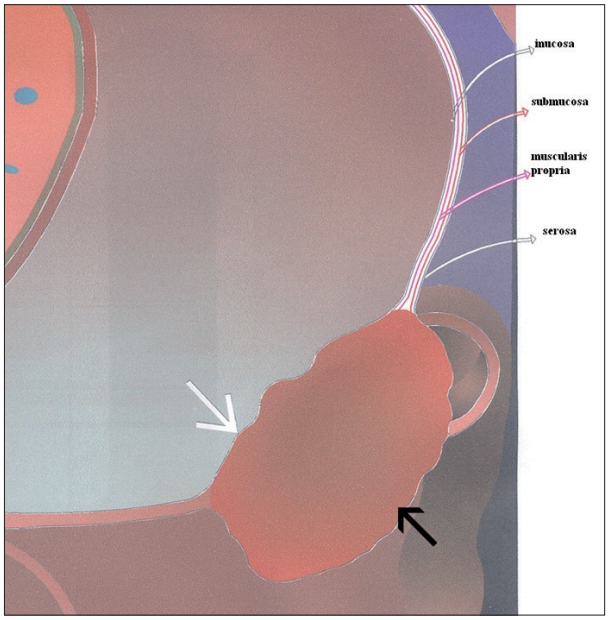

Figure 1. The growth pattern of gastrointestinal stromal tumors. White arrow indicates intraluminal portion, and black arrow shows extraluminal components of the tumor.

ed tomography (CT) features of malignant GISTs have been established: lesion size exceeding 5 cm diameter, irregular surface, indistinct margins, tissue invasion, heterogeneous contrast enhancement, hepatic metastases, and peritoneal dissemination. Metastatic lymphadenopathy is uncommon with this type of tumor (7–12).

The exact distribution of the GISTs is not clearly known. It is estimated that the frequency of GIST in the general population is 10 to 20 cases per million (2). Most patients are older than 50 years at the time of presentation. In young adults and children, GISTs are very rare and are sometimes associated with familial disorders, such as neurofibromatosis type 1 (13). The clinical presentations of these tumors vary according to their site and size. The size of the tumor ranges from 0.5 to 21 cm, with a mean of 6.8 cm. Imaging and

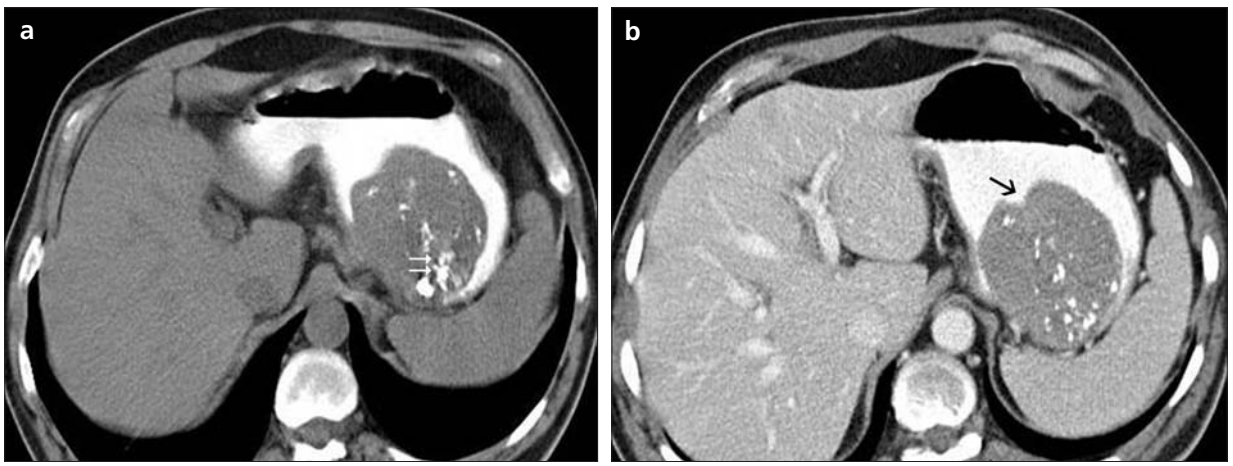

Figure 2. a, b. A 65-year-old man who presented with abdominal pain. Axial CT images **(a, b)** before **(a)** and after contrast-enhancement **(b)** show a heterogeneous soft-tissue mass involving the gastric wall, with calcification **(***white arrows,* **a)**. The black arrow **(b)** indicates ulceration of the overlying mucosa of the tumor.

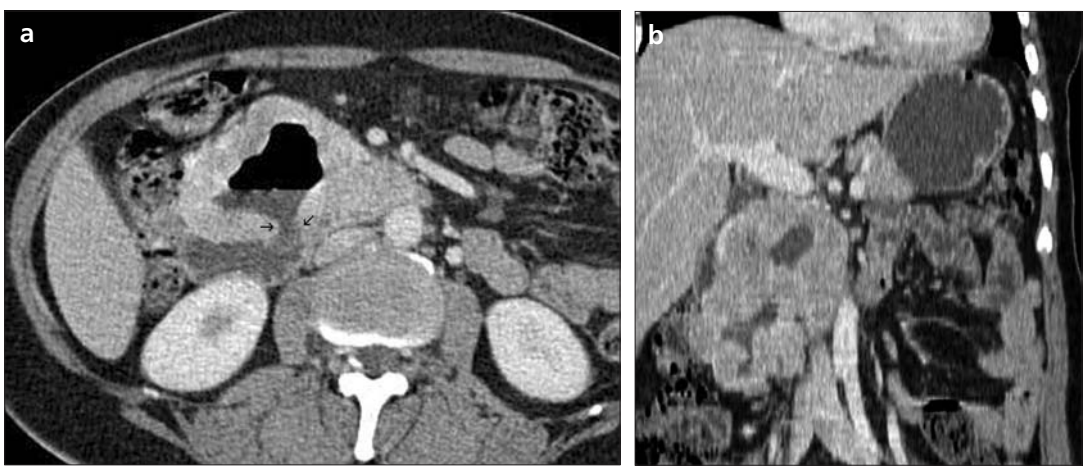

Figure 3. a, b. A 45-year-old woman who presented with gastrointestinal bleeding and abdominal pain. Contrast-enhanced axial **(a)** and coronal **(b)** CT images show a soft-tissue mass involving the muscularis propria of the second part of duodenum. The mass with cysts and cavity communicates with the duodenal lumen and contains air and air-fluid levels **(***arrows,* **a)**.

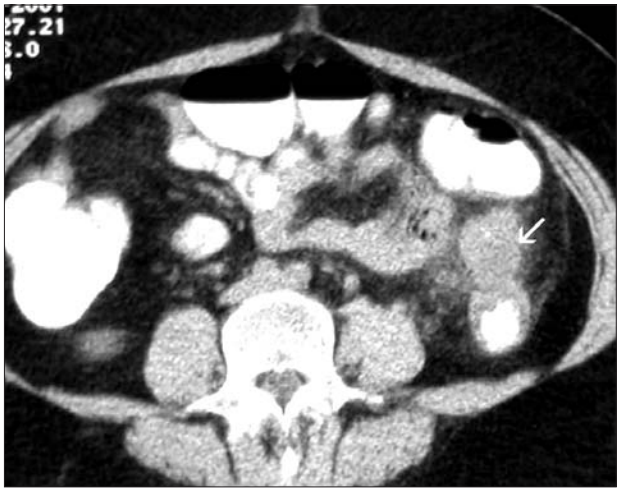

Figure 4. A 42-year-old woman who presented with left lower abdominal pain and tenderness. CT scan after contrast enhancement shows the primary mass originating from the wall of the descending colon with extraluminal growth *(white arrow)*.

Figure 5. A 55-year-old man who presented with abdominal pain and obstructive jaundice. CT scan after contrast enhancement shows the primary mass in the second part of the duodenum *(black arrows)* and the dilated common bile duct *(white arrow)* and pancreatic duct.

operative incidental findings are common. The most common presentation in symptomatic GISTs is gastrointestinal bleeding caused by ulceration of the overlying mucosa of the tumor. Patients may sometimes present with symptoms of anemia caused by occult bleeding (e.g., melena). Other clinical presentations are associated with the location of the tumor. For example, these symptoms may be nausea, vomiting, abdominal pain, obstructive jaundice (Fig. 5), and vague mass and abdominal distension.

Cross-sectional imaging findings

The most common location for GISTs is the stomach. The CT features of gastric GISTs are typical. CT scans show a large mass with solid or cystic components (Fig. 6). The tumor originates in the gastric wall and extends into the adjacent structures including the mesenteric fat plane, the gastrohepatic ligament, or the omentum. The adjacent organs and mesenteric fatty planes may be displaced where GISTs invade. CT also may show ascites where the tumor has spread into the omentum or peritoneal cavity; liver metastases may also be present. However, metastatic lymphadenopathy is not a common feature in patients with GISTs.

Magnetic resonance imaging (MRI) features of gastric GISTs vary, owing to the degree of necrosis and hemorrhage that affect the signal-intensity pattern. The solid components of the tumor generally appear as low signal intensities on T1-weighted images, and

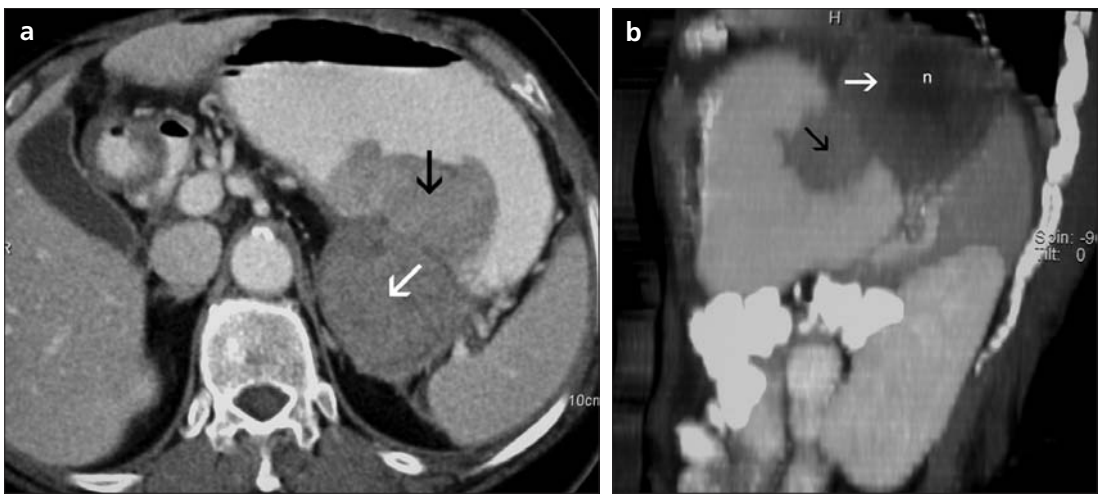

Figure 6. a, b. A 60-year-old man who presented with gastrointestinal bleeding and a palpable abdominal mass. The tumor originated in the muscularis propria and serosa of the stomach. Contrast-enhanced axial **(a)** and coronal reformatted **(b)** CT images show the same soft-tissue mass involving the muscularis propria of the stomach. Black arrows show the endoluminal component, white arrows show the extraluminal component (n, cystic/necrotic cavity).

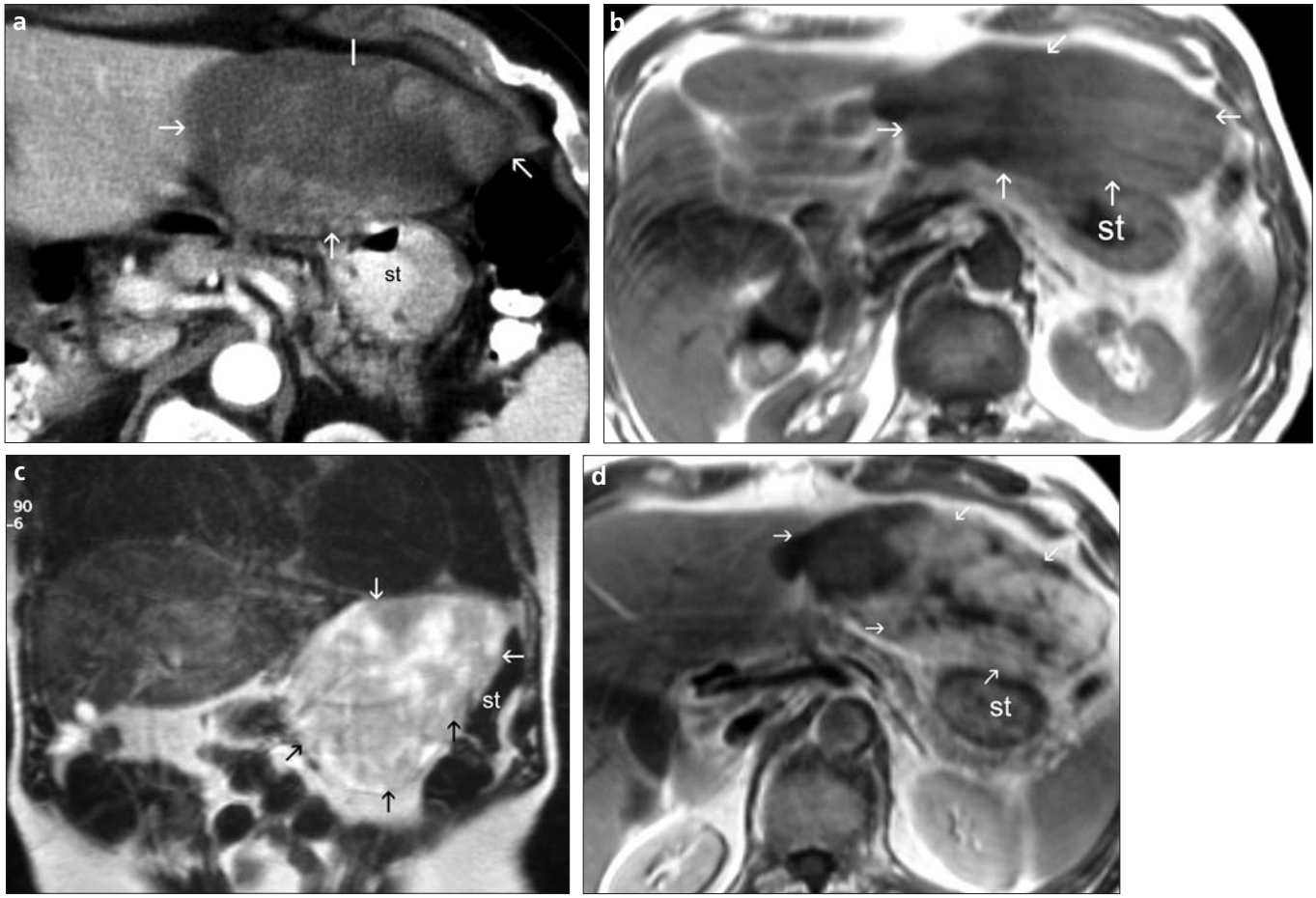

Figure 7. a–d. A 56-year-old man who presented with a palpable epigastric mass that originated in the stomach *(st)* wall. **(a)** Axial postcontrast CT, **(b)** axial T1-weighted, **(c)** coronal T2-weighted, and **(d)** axial postcontrast T1-weighted MR images show an epigastric mass *(arrows)* that included cystic and solid components and heterogeneous enhancement of the lesion. The mass is adjacent the left lobe of the liver.

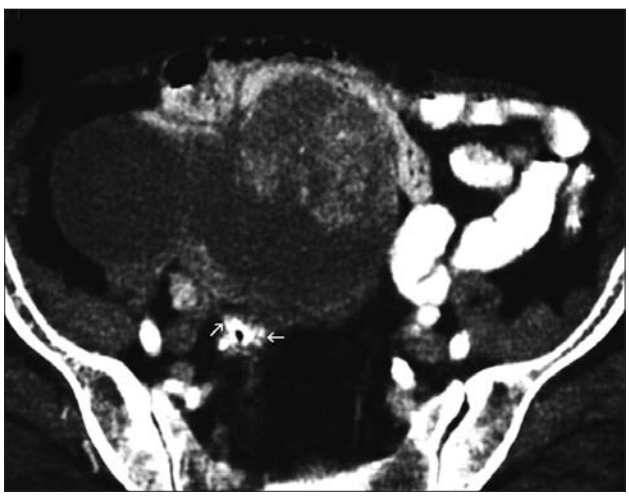

Figure 8. A 61-year-old woman who presented with a palpable pelvic mass. Contrast-enhanced axial CT image shows huge pelvic lesion (mimicking ovarian mass) and white solid components at the periphery of the cystic lesion involving the muscularis propria and serosa of ileum *(white arrows)*.

high signal intensities on T2-weighted images and after enhancement with gadolinium (Fig. 7). Depending on the age of the hemorrhage, portions of hemorrhage within the GIST vary from high to low signal intensity on both T1- and T2-weighted images.

In many cases, the extragastric or extraintestinal portion is so large that it is difficult to determine the origin of the tumor on the intestinal wall with CT or MR images (Fig. 8). The tumor is sometimes attached to the intestinal wall via a thin pedicle.

A peripheral solid-component enhancement pattern shows viable areas; central areas of low density correspond to hemorrhagic, cystic, or necrotic components. These cysts and cavities may communicate with the intestinal lumen and contain air, air-fluid levels, or oral contrast media (Fig. 3). Calcifications are rare features of GISTs. A GIST with a circumferential growth pattern is considered an aneurysmal dilatation of the affected colonic or small intestine segment (Fig. 9).

The differential diagnosis for GISTs should be made according to the tumor location. For example, the differential diagnosis of gastric GISTs must include other mesenchymal neoplasms such as leiomyomas, leiomyosarcomas, schwannomas, neurofibromas, and neuroendocrine neoplasms. The imaging findings of all of these neoplasms

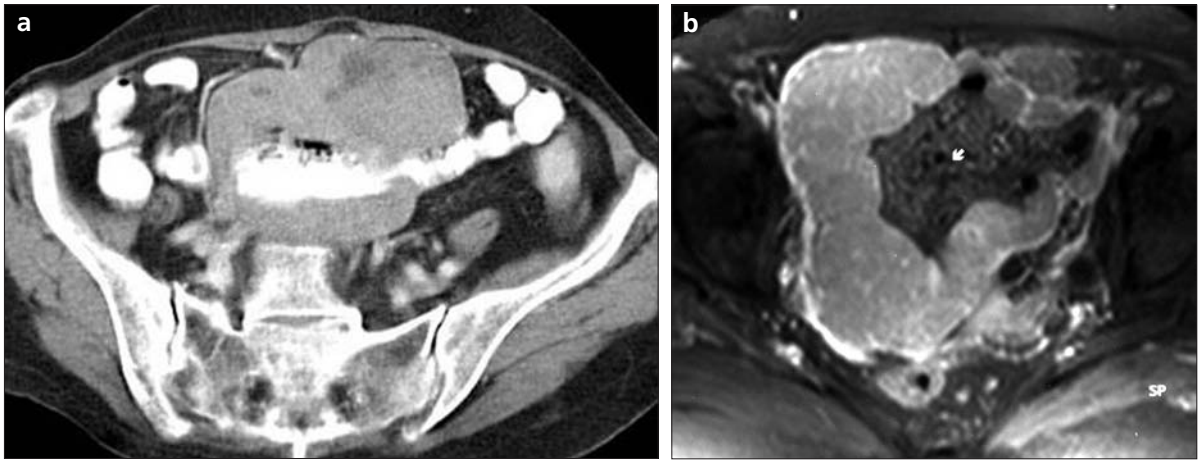

Figure 9. a, b. A 63-year-old woman who presented with abdominal pain. **(a)** Axial CT and **(b)** axial T2-weighted MR images show a heterogeneous soft-tissue mass involving the small bowel wall and causing saccular aneurysmal dilatation *(white arrow indicates dilated small bowel lumen)*.

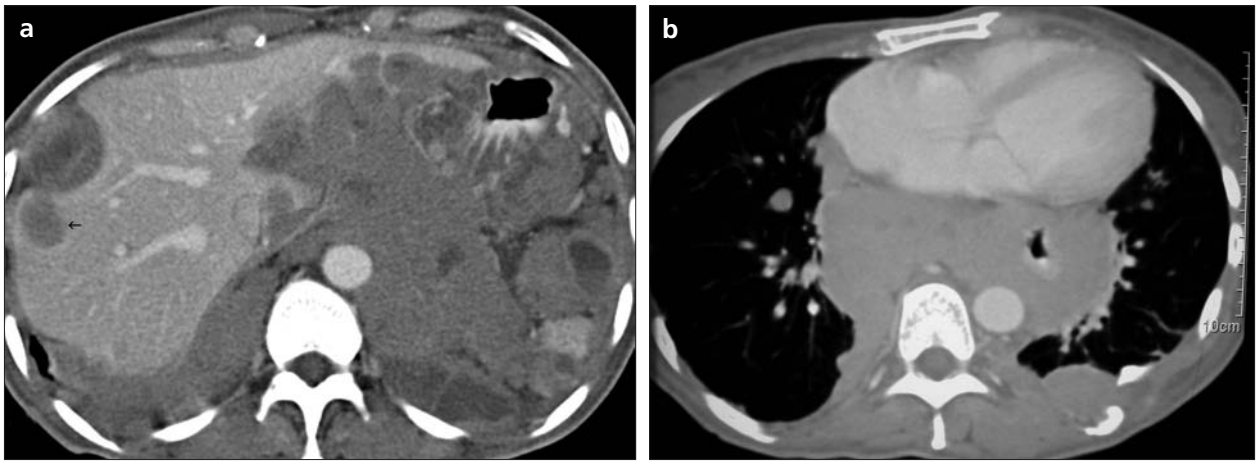

Figure 10. a, b. A 45-year-old man who presented with abdominal pain and a palpable mass that originated in the gastric wall. **(a)** Contrast-enhanced CT shows low-attenuation metastatic masses with peripheral enhancement in the peritoneum and liver *(black arrow)*. **(b)** Contrast-enhanced CT scan shows pleural and mediastinal metastases in addition to lung nodules.

are similar to GISTs because they, too, originate from the gastric wall.

Gastric adenocarcinomas and lymphomas also should be considered in the differential diagnosis of gastric GISTs. Although gastric carcinomas and lymphomas commonly have associated regional lymphadenopathy, lymphadenopathy is not a feature of malignant GISTs.

The differential diagnosis for GIST in the small intestine includes adenocarcinoma and lymphoma. The presence of associated lymphadenopathy is the most important clue for the diagnosis of lymphoma. Although anorectal and colonic GISTs are rare, the differential diagnoses of these tumors are similar to those of gastric and small bowel GISTs.

The most important complications of GIST are hemorrhage and spontaneous rupture into the peritoneal or endoluminal cavities caused by emergent laparotomies.

GISTs often metastasize to the liver and the peritoneum. However, pulmonary metastases are rarely seen. The CT or MRI appearance of metastases after the administration of intravenous (IV) contrast media generally correlates with the degree of tumor vascularity. On enhanced CT, most lesions appear as hypodense or isodense compared with the adjacent parenchyma, with the exception of retained hemorrhage, proteinaceous material, or calcifications (14) (Fig. 10).

The best therapy for patients with GISTs has been surgical resection of the tumor. Conventional chemotherapeutic agents and radiation are rarely effective against GISTs. Recently, a clinical trial of STI-571 (Gleevec®, Novartis, Basel, Switzerland), a first-generation tyrosine kinase inhibitor with high specificity for the tyrosine kinase c-KIT, was used for unresectable or metastatic disease. On follow-up CT, hepatic and peritoneal metastases showed significantly decreased attenuation and development of a cyst-like appearance. Gleevec® has proved to be a breakthrough drug with remarkable efficacy for treating metastatic GIST (14, 15). Understanding the unusual appearances of GISTs is important because radiologists can misinterpret cystic-appearing hypodense liver lesions after Gleevec® treatment as active disease (Fig. 11).

If CT scans are performed as single-phase studies, it is possible that hypervascular foci may be missed on the venous phase of the study. For this reason, MRI with gadolinium is better at detecting the internal structure, particularly the foci of hypervascularity of treated liver metastases (15). It is likely

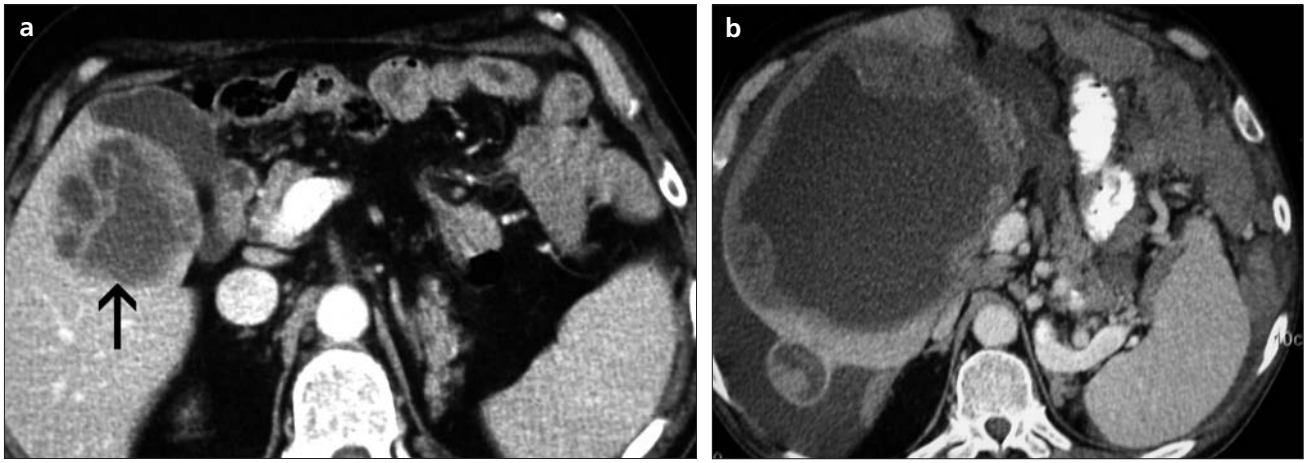

Figure 11. a, b. A 47-year-old man who presented with several hepatic metastases from GIST. Contrast-enhanced CT before Gleevec therapy **(a)** shows a 6×5 cm heterogeneous and a hypodense metastasis *(arrow)* with low density (45 HU). CT after 8 weeks of treatment with Gleevec **(b)** shows that the masses have become larger, with cystlike density (28 HU) and a well-defined border.

that contrast-enhanced MRI or dual-phase CT may be superior to single-phase CT in assessing disease response to Gleevec® therapy and identifying those at risk of relapse. Mesenteric metastases are better seen on CT than on MRI examination (3).

Gastrointestinal stromal tumors are mesenchymal tumors on the muscularis propria of the gastrointestinal tract wall. CT and MRI can be useful cross-sectional imaging modalities for the diagnosis, staging, and follow-up of patients with GISTs.

References

1. Hasegawa T, Matsuno Y, Shimoda T, et al. Gastrointestinal stromal tumor: consistent CD117 immunostaining for diagnosis, and prognostic classification based on tumor size and MIB-1 grade. Hum Pathol 2002; 33:669–676.
2. Miettinen M, El-Rifai W, Sobin LH, et al. Evaluation of malignancy and prognosis of gastrointestinal stromal tumors: a review. Hum Pathol 2002; 33:478–483.
3. Sandrasegaran K, Rajesh A, Rushing DA, et al. Gastrointestinal stromal tumors: CT and MRI findings. Eur Radiol 2005; 15:1407–1414.
4. Kim HC, Lee JM, Kim KW, et al. Gastrointestinal stromal tumors of the stomach: CT findings and prediction of malignancy AJR Am J Roentgenol 2004; 183:893–898.
5. Burkill GJ, Badran M, Al-Muderis O, et al. Malignant gastrointestinal stromal tumor: distribution, imaging features, and pattern of metastatic spread Radiology 2003; 226:527–532.
6. Hornick JL, Fletcher CD. The role of KIT in the management of patients with gastrointestinal stromal tumors. Hum Pathol 2007; 38:679–687.
7. Tateishi U, Hasegawa T, Satake M, et al. Gastrointestinal stromal tumor correlation of computed tomography findings with tumor grade and mortality. J Comput Assist Tomogr 2003; 27:792–798.
8. Levy AD, Remotti HE, Thompson WM, et al. Gastrointestinal stromal tumors: radiologic features with pathologic correlation Radiographics 2003; 23:283–304.
9. Hersh MR, Choi J, Garrett C, et al. Imaging gastrointestinal stromal tumors. Cancer Control 2005; 12:111–115.
10. Lau S, Tam KF, Kam CK, et al. Imaging of gastrointestinal stromal tumour (GIST). Clin Radiol 2004; 59:487–498.
11. Lee CM, Chen HC, Leung TK, Chen YY. Gastrointestinal stromal tumor: computed tomographic features. World J Gastroenterol 2004; 10:2417–2418.
12. Hortan KM, Juluru K, Montogomery E, et al. Computed tomography imaging of gastrointestinal stromal tumors with pathology correlation. J Comput Assist Tomogr 2004; 28:811–817.
13. Behrenwala KA, Spalding D, Wotherspoon A, Fisher C, Thompson JN. Small bowel gastrointestinal stromal tumours and ampullary cancer in Type I neurofibromatosis. World J Surg Oncol 2004; 7:1–4.
14. Chen MYM, Bechtold RE, Savage PD. Cystic changes in hepatic metastases from gastrointestinal stromal tumors (GISTs) treated with Gleevec (imatinib mesylate). AJR Am J Roentgenol 2002; 179:1059–1062.
15. Bechtold RE, Chen MY, Stanton CA, Savage PD, Levine EA. Cystic changes in hepatic and peritoneal metastases from gastrointestinal stromal tumors treated with Gleevec. Abdom Imaging 2003; 28:808–814.